JOURNAL OF AIRCRAFT
Vol. 40, No. 4, July–August 2003

Design of Low Reynolds Number Airfoils with Trips

Ashok Gopalarathnam*
North Carolina State University, Raleigh, North Carolina 27695
and
Benjamin A. Broughton,† Bryan D. McGranahan,‡ and Michael S. Selig§
University of Illinois at Urbana–Champaign, Urbana, Illinois 61801

A design philosophy for low Reynolds number airfoils that judiciously combines the tailoring of the airfoil pressure distribution using a transition ramp with the use of boundary-layer trips is presented. Three airfoils with systematic changes to the shape of the transition ramp have been designed to study the effect of trips on the airfoil performance. The airfoils were wind-tunnel tested with various trip locations and at Reynolds numbers of 100,000 and 300,000 to assess the effectiveness of the design philosophy. The results show that the design philosophy was successfully used in integrating a boundary-layer trip from the outset in the airfoil design process. For the Reynolds numbers and the range of airfoil shapes considered, however, airfoils designed with trips do not hold any clear advantage over airfoils designed for good performance in the clean condition.

Nomenclature

C_d = airfoil drag coefficient based on the chord
C_f = local skin-friction coefficient
C_l = airfoil lift coefficient based on the chord
C_m = airfoil pitching moment coefficient about the quarter-chord location
c = airfoil chord
Re = Reynolds number based on the chord
V = airfoil surface velocity
V_∞ = freestream velocity
x = chordwise coordinate
α = angle of attack

Subscripts

r = bubble reattachment location
s = laminar separation location
tr = transition location

Introduction

IT is well known that for an airfoil to achieve low drag in a low Reynolds number ($60{,}000 < Re < 500{,}000$) environment, it is important to eliminate or reduce the drag caused by the laminar separation bubble, referred to here as "bubble drag." One of the ways of reducing the bubble drag is by the use of a transition ramp,[1–7] which is the long region of adverse pressure gradient used to destabilize the laminar boundary layer and promote transition while avoiding large transitional bubbles. The shape of the transition ramp is also closely associated with the variation of the chordwise transition location x_{tr}/c with lift coefficient C_l. The larger the change in the x_{tr}/c for a given change in C_l, the shallower is the transition curve, and the lower is the bubble drag. Although a shallower transition curve results in lower bubble drag, it also results in a smaller C_l range over which this low drag can be achieved. Thus, the designer has to make a tradeoff between a decrease in the bubble drag and the C_l range over which this low drag is achieved.[3]

A second means of reducing bubble drag is by the use of boundary-layer trips to completely eliminate or at least reduce the intensity of the laminar bubble.[8,9] Trips are often used to improve the performance of an airfoil that has a large bubble drag in the clean configuration.[5,10–20] Owing to the difficulties in predicting the effects of trips even on flat-plate boundary layers,[21,22] the use of trips on low Reynolds number airfoils has primarily relied on trial-and-error approaches along with wind-tunnel testing[15–19] or flight testing.[20] The difficulty with designing low Reynolds number airfoils with upper-surface trips is that a trip configuration that is beneficial for one airfoil angle of attack and Reynolds number might be detrimental for some other operating condition. These tradeoffs are also highly dependent on the bubble size, intensity, and their variation with airfoil angle of attack, making the effectiveness of a trip very much airfoil dependent.

In an effort to better understand the effectiveness of trips in controlling the bubble drag on low Reynolds number airfoils, a systematic experimental investigation[13] was conducted in the University of Illinois at Urbana–Champaign in 1997. A variety of single and multiple trip configurations were studied and their effects on three low Reynolds number airfoils were quantified in a series of wind-tunnel experiments. Surface oil-flow visualization was also performed for these cases in order to determine the causal factors for the measured changes in the airfoil drag. Over a Reynolds number range of 100,000 to 300,000 the study examined the trips effects on three airfoils that had progressively less bubble drag: M06-13-128, E374, and SD7037. Each airfoil was considered at a single angle of attack corresponding to the middle of the drag polar of the corresponding airfoil, and the investigation focused on the drag benefit from each trip configuration and chordwise location relative to the clean airfoil. The results from the study showed that for the Reynolds numbers and airfoils considered, 1) there is little advantage in using multiple two-dimensional trips or complex three-dimensional trips over single two-dimensional trips; 2) dramatic drag reductions are seen for relatively thin trips, with thicker trips having only incrementally better performance; 3) the chordwise location of the trip had little effect on the drag as long as the trip is positioned upstream of the laminar separation; and 4) at the single angle of attack considered

Presented as Paper 2001-2463 at the 19th AIAA Applied Aero Conference; received 14 September 2002; revision received 21 April 2003; accepted for publication 24 April 2003.

*Assistant Professor, Department of Mechanical and Aerospace Engineering, Box 7910; ashok_g@ncsu.edu. Member AIAA.
†Graduate Research Assistant, Department of Aeronautical and Astronautical Engineering, 306 Talbot Laboratory, 104 S. Wright Street; bbrought@uiuc.edu. Student Member AIAA.
‡Graduate Research Assistant, Department of Aeronautical and Astronautical Engineering, 306 Talbot Laboratory, 104 S. Wright Street; mcgranah@uiuc.edu. Student Member AIAA.
§Associate Professor, Department of Aeronautical and Astronautical Engineering, 306 Talbot Laboratory, 104 S. Wright Street; m-selig@uiuc.edu. Senior Member AIAA.

for each airfoil, it was not possible to improve the performance of an airfoil with a large separation bubble using trips to have less drag than an untripped airfoil with a small bubble.

The current work extends the systematic study in Ref. 13 by considering three airfoils designed specifically for this study with systematic changes to the upper-surface transition ramp and by considering the trip effects on the entire drag polar instead of at just one angle of attack. Using the results of the previous work,[13] the current study uses just a single trip configuration: a simple two-dimensional trip of a single thickness. Although the results from the previous work showed the relative insensitivity of the drag to trip location upstream of the laminar separation, the chordwise location of the trip has been varied in the current study because of the variation in the chordwise location of the separation bubble that accompanies changes in airfoil angle of attack.

The primary objective of the current work is to develop a philosophy for the design of low Reynolds number airfoils that integrates the use of trips from the beginning in the airfoil design process. The key idea is to judiciously combine the use of a transition ramp to achieve low bubble drag over one portion of the drag polar and to use boundary-layer trips to extend the C_l range over which low bubble drag is obtained. An aim of the work is to determine whether an airfoil designed to use trips will have a better performance overall than one designed for good performance when clean. The performance comparison in this study extends over a large C_l range as opposed to a single C_l considered in the earlier work.[13]

The following section briefly describes the two common approaches to achieving low bubble drag, namely, the use of 1) transition ramps and 2) boundary-layer trips. The design philosophy developed in the current work to integrate trips in the airfoil design process is then described. Experimental results are then presented to demonstrate the effectiveness of the design philosophy. Results for three airfoils are presented both with and without boundary-layer trips on the upper surface. The three airfoils have been designed with systematic changes to the shape of the transition ramp with the specific objective of studying trip effects.

Means of Achieving Low Bubble Drag

As described earlier, there are two common means used to achieve low bubble drag on airfoils operating at low Reynolds numbers: 1) by tailoring the transition curve (transition ramp) and 2) by use of boundary-layer trips. In this section these two methods will be examined briefly to understand how they affect the size of the bubble and the resulting drag.

Effect of the Transition Curve on Drag

The effect of the transition curve is demonstrated using two example airfoils A and B adapted from Ref. 7. Figure 1 shows a comparison of the geometries and inviscid velocity distributions for the two airfoils. These airfoils were designed using PROFOIL,[23,24] a multipoint inverse airfoil design method based on conformal mapping.

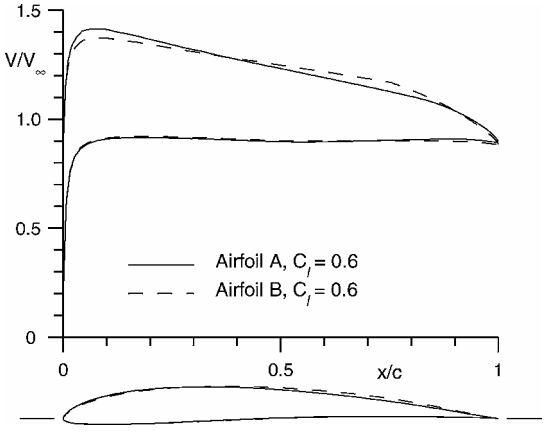

Fig. 1 Inviscid velocity distributions for airfoils A and B to study the different effects on drag.

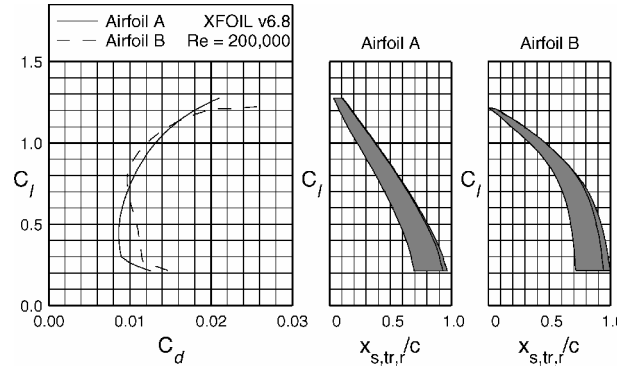

Fig. 2 XFOIL predictions for airfoils A and B to illustrate the effects of changes in the transition ramp on drag.

The two airfoils were designed to have two different shapes for the transition ramp on the upper surface. The airfoils were then analyzed using XFOIL,[25] a viscous design/analysis method for single-element airfoils. In this and all of the other XFOIL results presented in this work, a value of $n_{\text{crit}} = 9$ has been assumed for the critical transition amplification factor, and unless otherwise mentioned all of the analyses have been conducted using the free-transition option in which the code computes the transition location as a part of the solution procedure. Figure 2 shows the drag polars and upper-surface transition curves for a Reynolds number of 200,000. For the sake of this discussion, the transition ramp is defined here as the region over which the bubble moves gradually as defined by the transition curve.

From Fig. 2 it can be seen that airfoil A has lower drag than airfoil B at lift coefficients from around 0·3 to around 0·7, above which airfoil B has lower drag. Also noticeable is the correlation between the drag polar and the shape of the upper-surface transition curve. For the C_l range from 0.3–0.7, where airfoil A has lower drag, the transition curve for airfoil A is shallower than for airfoil B. That is, there is a larger change in the value of x_{tr} for airfoil A than for B over this C_l range. For values of C_l from 0.7–1.2 where airfoil B has lower drag, the transition curve for airfoil B is shallower than for A. This figure shows that the steepness of the transition curve is a direct indication of the bubble drag. By adjusting the shape of this curve, it is possible to tailor the drag polar of an airfoil at low Reynolds numbers.

Figure 2 also includes an overlay of the variation of bubble size $(x_r - x_s)$ with C_l. The size of the bubble for each C_l was obtained by determining the chordwise extent over which the local skin-friction C_f, as predicted by XFOIL, was less than or equal to zero. Studying the bubble-size variation for the two airfoils further illustrates the connection between the shape of the transition curve and the bubble drag. The bubble is larger when the transition curve is steeper.

Figure 3 shows the inviscid velocity distributions for airfoil A at C_l values of 0.5 and 1.0 with the upper-surface bubble location marked in bold. A similar plot for airfoil B is shown in Fig. 4. Comparing the velocity drops across the bubble for the four cases, it can be seen that while airfoil A has a smaller velocity drop than airfoil B at $C_l = 0.5$ the situation is reversed for $C_l = 1.0$. Because the pressure drag caused by the bubble increases with increasing velocity drop across the bubble, airfoil A has smaller bubble drag at the low C_l and larger bubble drag at the higher C_l. Thus, a steeper transition curve results in a larger bubble and also larger velocity drop across the bubble causing an increase in bubble drag.

Effect of the Trips on Drag

Trips have been widely used[5,8–20] to improve performance of airfoils having high bubble drag. As described in Refs. 13 and 14, trips (when properly designed) can cause a net reduction in the drag as a consequence of three main effects: a reduction in bubble drag, added device drag, and an increase in skin-friction drag. Figure 5, taken from Refs. 13 and 14, shows how the cumulative result of these three effects can reduce the overall drag at a particular C_l. Clearly, a trip configuration can be effective only when the decrease in bubble

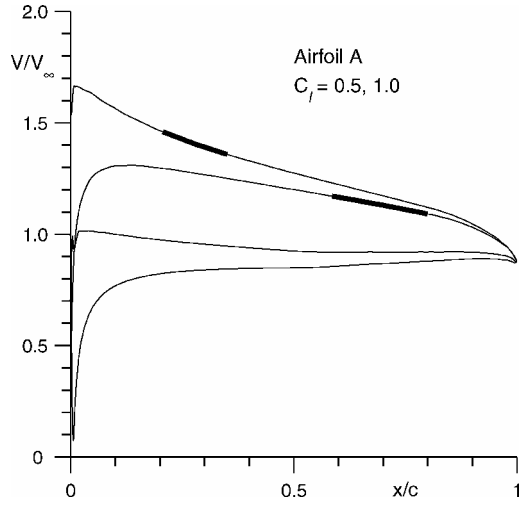

Fig. 3 Inviscid velocity distributions for airfoil A with the locations of the bubble marked.

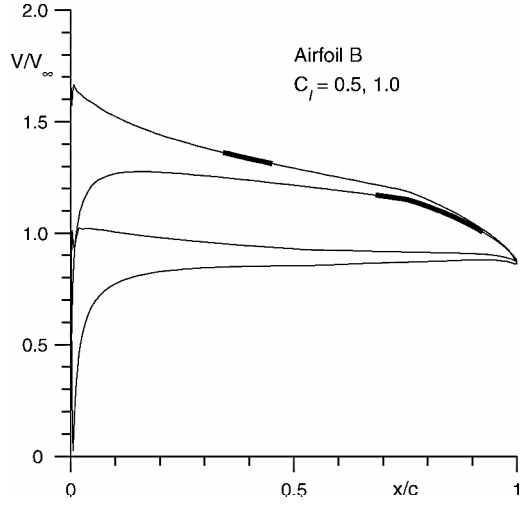

Fig. 4 Inviscid velocity distributions for airfoil B with the locations of the bubble marked.

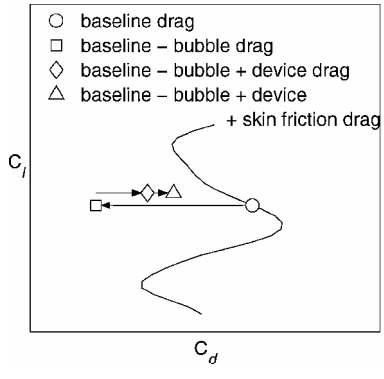

Fig. 5 Conceptual illustration of trip effects.[13,14]

drag is significantly greater than the added device drag caused by protuberance effects of the trip and the added skin friction caused by loss in laminar flow. Because of the fact that the bubble location varies with airfoil angle of attack and the bubble drag varies with Reynolds number, a trip configuration and location that is well suited for one flight condition might be ineffective or even detrimental for another condition. Figure 6 shows an example where the use of trips has resulted in significant drag reductions over a large C_l range for an airfoil having large bubble drag.

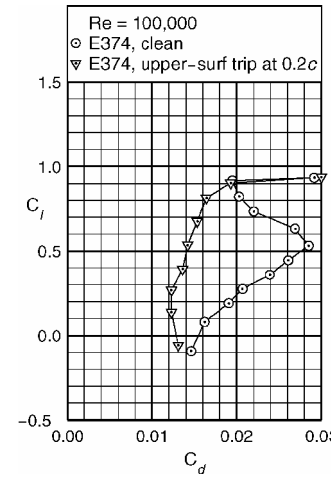

Fig. 6 Effect of a trip on the E374 polar at $Re = 100{,}000$ (data from Ref. 10).

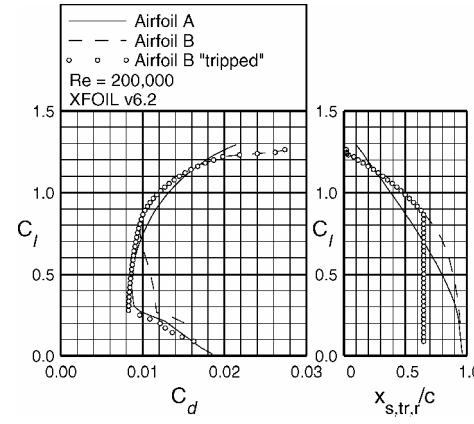

Fig. 7 Effect of fixing transition on the upper surface of airfoil B, as predicted by XFOIL.

Design Philosophy for Airfoils with Trips

To illustrate the philosophy for designing airfoils to use trips from the outset to achieve good performance, the two airfoils A and B from the preceding section are reconsidered. As seen from Fig. 2, airfoil B has lower drag at the higher C_l values and has higher drag at the lower C_l values. As discussed earlier, the higher drag for B at the lower C_l values is associated with the steeper transition curve for this airfoil at these C_l values. A question can now be posed: Would it be possible to extend the low-drag behavior that airfoil B achieves at high C_l values to lower C_l conditions by using a boundary-layer trip to reduce the intensity of the bubble at the lower values of C_l, and would such a trip configuration result in a performance that is better overall than that of airfoil A?

To explore this option in greater depth, XFOIL was used to study the effect of fixing the upper-surface transition location on airfoil B. Figure 7 compares the resulting drag polar with those for the clean airfoils A and B. As seen from the figure, the performance of airfoil B with transition fixed at 65%c on the upper surface is superior to those of the clean airfoils A and B. It must be remembered, however, that when analyzing an airfoil using XFOIL with fixed transition at a specified location, XFOIL assumes instantaneous transition from laminar to turbulent flow at that point and results in complete elimination of any bubble that might have otherwise occurred downstream of that point. In reality, however, the disturbance resulting from trips on low Reynolds number airfoils does not always cause instantaneous transition at the trip location. As the experimental results of Ref. 13 show, trips on airfoils at low Reynolds numbers often need to be located several tenths of chord upstream of a bubble to significantly diminish the bubble intensity. Many trip configurations are also unsuccessful in completely eliminating the bubble. Also no device drag is assumed in the XFOIL when fixing transition.

In spite of the limitations of XFOIL in accurately modeling boundary-layer trips, the results in Fig. 7 do provide confidence that a judicious combination of the transition ramp and a boundary-layer trip can result in an airfoil having a better performance overall than one designed for good performance when clean. The results from Fig. 7 also show that an airfoil designed for use with trips will need to have the transition ramp tailored so that it results in low drag at the higher values of C_l with a shallow slope for the transition curve at these values of C_l. The consequence of a shallow transition curve at the high C_l conditions is that the curve ends up with a steep slope at the low C_l conditions. As a result, such an airfoil has large bubble drag at the low C_l conditions. The boundary-layertrip, located on the upper surface at a forward location can be used to diminish the bubble at low values of C_l and "extend" the low drag achieved at the high values of C_l. The design philosophy, therefore, involves tailoring of the transition ramp to result in low C_d at the high-C_l conditions via the use of a shallow transition-curve slope and combining it with the use of boundary-layer trips to avoid the large bubble drag associated with the steep transition-curve slope that results at the lower C_l conditions. Owing to the fact that there are no readily available computer programs that can accurately predict the effect of trips, experimental studies need to be made to determine the optimum trip location as well as the effectiveness of the design philosophy.

Experimental Investigation

In an effort to better understand the tradeoffs involved in designing airfoils that judiciously combine the effect of the transition ramp and a boundary-layer trip, three airfoils were designed using PROFOIL[23,24] specifically for this study with systematically varying transition ramps on the upper surfaces. Figure 8 shows the three airfoils SA7024, SA7025, and SA7026 and inviscid velocity distributions at a C_l of 0.6. Figures 9 and 10 show the predicted performance for the three airfoils at Reynolds numbers of 100,000 and 300,000. The systematic variations in the transition ramps (i.e., shapes of the x_{tr}/c curves) for the three airfoils are clearly seen. One of the design objectives was that the extents of the low-drag ranges of these airfoils should be similar. For this objective to be satisfied in combination with the fact that the three airfoils have different transition-ramp shapes, it was necessary to design the three airfoils to have three different thicknesses. As a result, the SA7024, SA7025, and the SA7026 have maximum thickness-to-chord ratios of 7, 8, and 9%, respectively.

Only a brief description of the experimental apparatus is provided here; more details are available in Refs. 11, 12, and 14. The

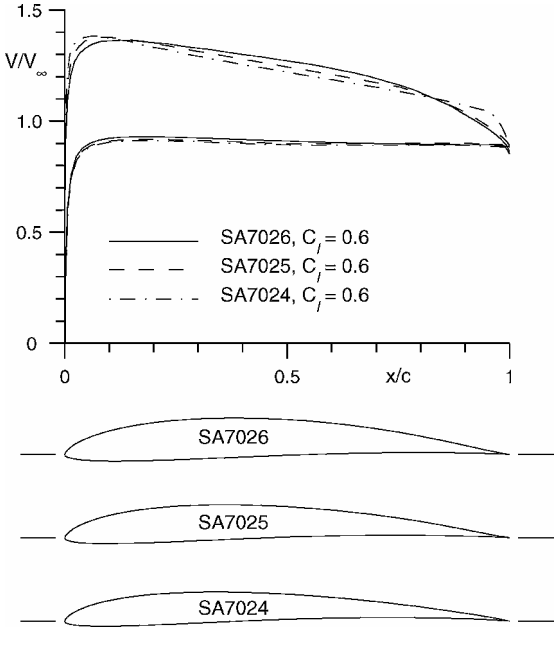

Fig. 8 SA702x airfoils and inviscid velocity distributions.

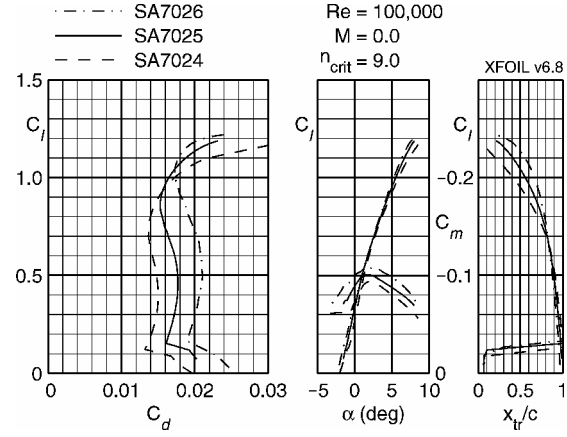

Fig. 9 XFOIL predictions for the SA702x airfoil series at *Re* of 100,000.

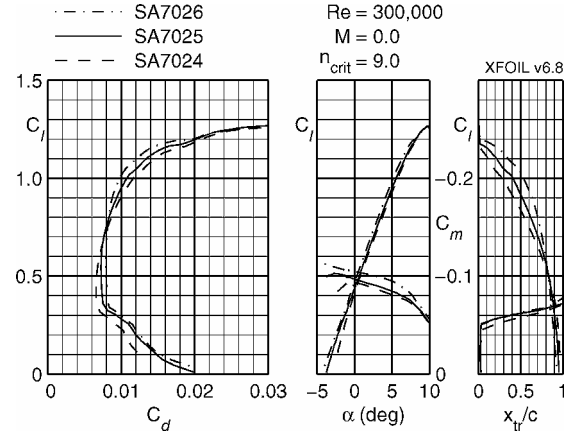

Fig. 10 XFOIL predictions for the SA702x airfoil series at *Re* of 300,000.

experiments were performed in the University of Illinois open-return subsonic wind tunnel. The rectangular test-section dimensions are approximately 2.8 $\times$ 4 ft in cross section and 8-ft long. To ensure good flow quality in the test section, the tunnel settling chamber contains a 4-in.-thick honeycomb and four antiturbulence screens, resulting in a turbulence level of less than 0.1% over the Reynolds number range tested.[11] The airfoil models were machined from polyurethane RenShape® using a numerically-controlled machine, structurally reinforced, then sanded and painted.

To isolate the ends of the airfoil model from the tunnel sidewall boundary layers and the outer support hardware, the airfoil models were mounted horizontally between two 3/8-in.-thick, 6-ft-long Plexiglas® splitter plates. Gaps between the model and splitter plates were nominally 0.05 in. All models had a 12-in. chord and 33 5/8-in. span. One side of the model was free to pivot. At this location the angle of attack was measured using a potentiometer. The other side of the model was free to move vertically on a precision ground shaft, but it was not free to rotate. A load cell restrained the motion of the model and measured the lift force. Linear and spherical ball bearings within the lift carriage helped to minimize any frictional effects.

The drag was obtained from the momentum method. To ensure that the wake had relaxed to tunnel static pressure, the wake measurements were performed 14.8 in. (approximately 1.25 chord lengths) downstream of the model trailing edge. Each vertical wake traverse consisted of between 20 and 80 total-head pressure measurements (depending on the wake thickness) with points nominally spaced 0.08 in. apart. Owing to spanwise wake nonuniformities,[26,27] wake-profile measurements were taken at several spanwise locations over the center of the model span. For the wake measurements made at the lower Reynolds number of 100,000, eight spanwise locations spaced 1.5 in. apart were used. At the higher Reynolds number of

300,000, the wake traverse measurements were made at four spanwise locations spaced 4 in. apart. In either case, the resulting drag coefficients were then averaged to obtain the drag at a given angle of attack.

The lift, drag, and angle-of-attack measurements were corrected to account for the effects of solid blockage, wake blockage, and streamline curvature.[28] The velocity was not only corrected for solid and wake blockage but also for a "circulation effect" that is unique to setups that make use of splitter plates. For the current tests the freestream velocity rather than being measured far upstream was measured between the splitter plates for higher accuracy. Because the pitot-static probe that was used to measure the freestream velocity was located fairly close to the model, the probe measurements were therefore corrected for airfoil circulation effects so as to obtain the true freestream test-section speed. The details of this correction procedure can be found in Ref. 29.

Overall uncertainty in the lift coefficient is estimated to be 1.5%. The drag measurement error comes from three sources: accuracy of the data-acquisition instruments, repeatability of the measurements, and the locations of the particular wake profiles used to determine the average drag coefficient. Based partly on the error analysis method presented in Refs. 30 and 31, the uncertainty caused by the instruments and measurement repeatability are less than 1 and 1.5%, respectively. Based on a statistical analysis (for a 95% confidence interval) of the spanwise drag results for the E374 airfoil[26] at $\alpha = 4$ deg, the uncertainties caused by the spanwise variations were estimated to be approximately 1.5% at and above $Re = 200{,}000$. The current airfoils are expected to have approximately the same uncertainties. A more detailed discussion of this topic is presented in Ref. 27. For the angle-of-attack sensor, the uncertainty is estimated to be 0.08 deg.

To determine the accuracy of airfoil profiles, each model was digitized with a Brown and Sharpe coordinate measuring machine. Approximately 80 points were taken around each airfoil, and the spacing between points was approximately proportional to the local curvature. Thus, near the leading and trailing edges, the spacing was relatively small, whereas over the midchord it was no greater than 0.7 in. These measured coordinates were compared with the true coordinates using a two-dimensional least-squares approach (rotation and vertical translation), which yielded an average difference of approximately 0.010 in. or less for all airfoils discussed in this paper.

Data taken on the E387 model for Reynolds numbers of 200,000 and 460,000 are presented in Ref. 11 and compare well with data taken in the NASA Langley Low-Turbulence Pressure Tunnel (LTPT).[30] Moreover, surface oil-flow visualization taken to determine the laminar separation and oil-accumulation lines showed that the lines agreed with NASA Langley LTPT data to within 1–2% of chord.[13] This good agreement serves to validate the current experiments.

Experimental Results

In this paper the experimental results are presented for the airfoils SA7024, SA7025, and SA7026 at Reynolds numbers of 100,000 and 300,000 and for five conditions: clean, trip at 0.1c, trip at 0.2c, trip at 0.3c, and trip at 0.4c.

All of the boundary-layer trips used in this study were constructed by using multiple layers of pressure-sensitive graphic tape, resulting in a total thickness of 0.0135 in. and a width of 0.125 in. They were placed on the airfoil such that the aft end of the tape was at the specified x/c location on the upper surface. In all cases the trips used were placed on the upper surfaces of the airfoil, and the lower surface was left clean.

In this section the experimental results for three airfoils in the clean condition are first presented. These results serve to compare experimental data with the XFOIL predictions. Next a matrix of drag polars is presented for the three airfoils and the four trip locations. In each polar plot the drag polars for that airfoil and trip location at Reynolds numbers of 100,000 and 300,000 are compared with the polars for the same airfoil in the clean condition at these Reynolds numbers. This matrix of polars allows comparison of drag for a given airfoil and different trip locations as well as for a given trip location for the three different airfoils. The last subsection then presents a comparison of the performance between the clean SA7024 and the tripped SA7026 in order to assess the design philosophy of designing an airfoil optimized for tripped performance to outperform an airfoil optimized for clean performance.

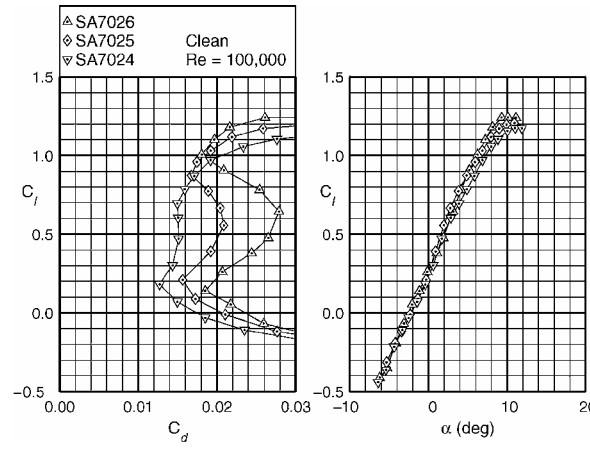

Fig. 11 Clean drag polars for $Re = 100{,}000$.

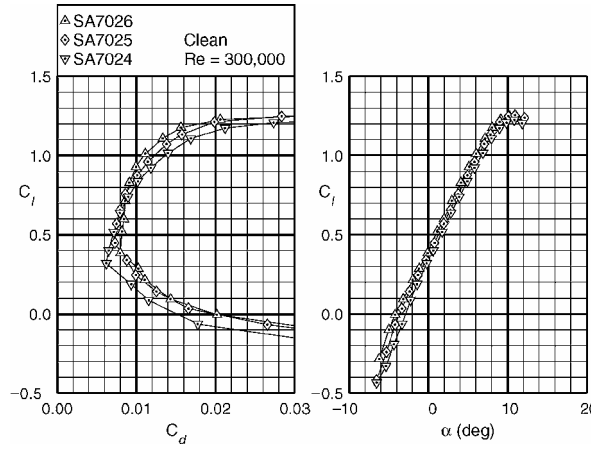

Fig. 12 Clean drag polars for $Re = 300{,}000$.

Results with No Trip

Figures 11 and 12 show the experimental results for the three airfoils at Reynolds numbers of 100,000 and 300,000. Comparing the results in these figures with the XFOIL predictions in Figs. 9 and 10, it is clear that the trends between the predictions compare well with those seen in the experiments. It is also seen that the design objectives have been satisfied. Comparison of the results for $Re = 100{,}000$ between the predictions and the experiments shows that XFOIL predicts lower drag in the portions of the polars where bubble drag is dominant. In the present study, however, the XFOIL code has been primarily used as an analysis tool to design airfoils with systematic variations in performance, and not necessarily with an aim of accurately predicting the absolute performance of each airfoil.

Comparison of Drag Polars

Figures 13–15 show the comparison of the tripped-airfoil performance with that of the clean airfoil for the two Reynolds numbers of 100,000 and 300,000 for the three SA702x airfoils. All four trip locations have been considered.

Comparison of the tripped-airfoil polars for the SA7024 in Figs. 13a–13d for $Re = 100{,}000$ shows that all of the four trip locations are in general equally effective at reducing the bubble drag as compared with the clean case. At $C_l = 0.4$, the 0.3c and 0.4c trip locations result in an approximately 0.002 greater reduction in

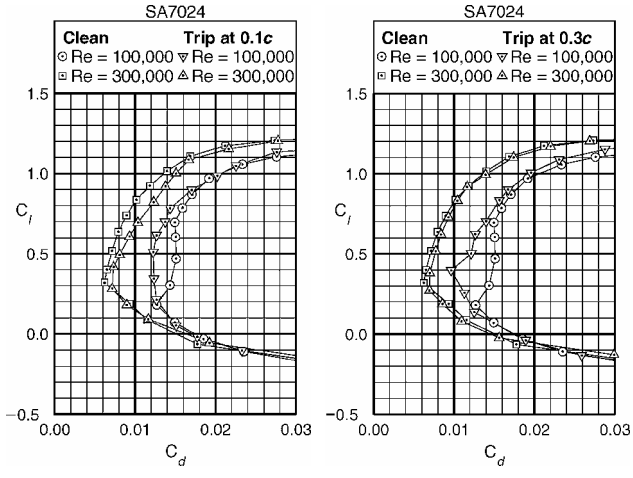

a) Trip at 0.1*c* c) Trip at 0.3*c*

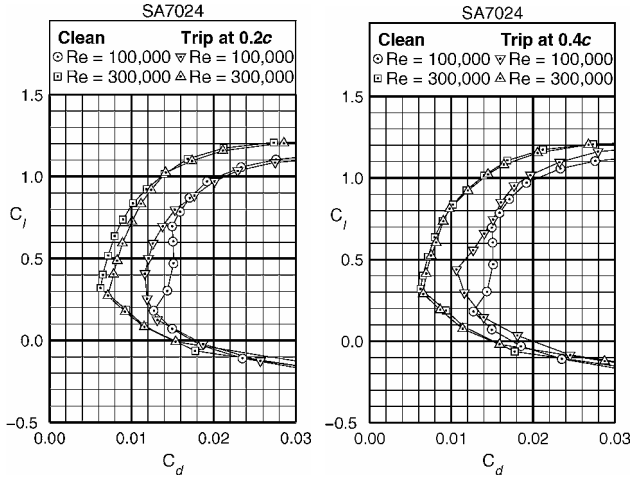

b) Trip at 0.2*c* d) Trip at 0.4*c*

Fig. 13 Drag polars for the SA7024.

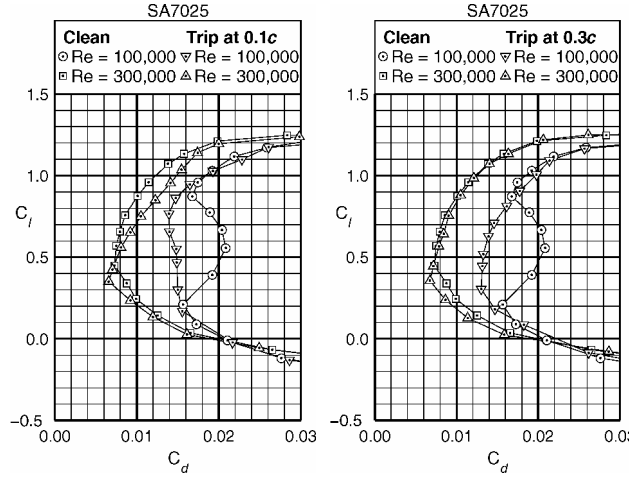

a) Trip at 0.1*c* c) Trip at 0.3*c*

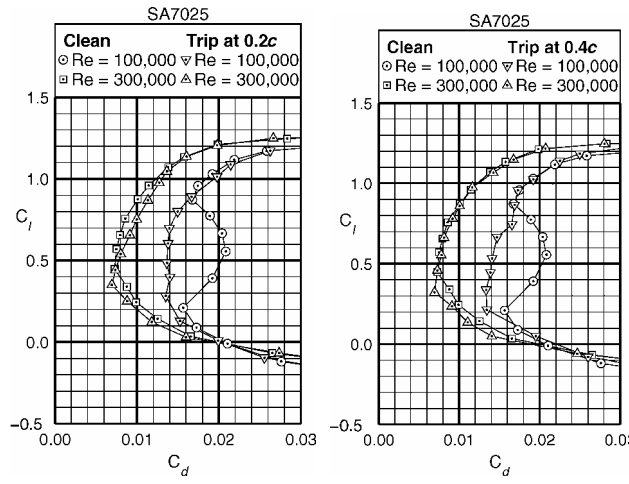

b) Trip at 0.2*c* d) Trip at 0.4*c*

Fig. 14 Drag polars for the SA7025.

C_d as compared with the more forward trip locations. At the higher Reynolds number of 300,000 there is clear increase in C_d for the 0.1*c* and 0.2*c* cases relative to the clean airfoil at C_l around 0.75. This increase in drag decreases progressively with aft movement of the trip location and can be attributed to increasing amounts of laminar flow with the aft movement of the trip location. The optimum location of the trip for the SA7024 airfoil is at 0.4*c*. At this location there is a reduction in drag around C_l of 0.4 at $Re = 100{,}000$. Although there is small increase in C_d around $C_l = 0.1$ at $Re = 100{,}000$, the airfoil on an airplane wing operates at higher Reynolds numbers at lower C_l values, and hence it can be expected that at $C_l = 0.1$ the operating Reynolds number will be closer to 300,000.

Figures 14a–14d present the results for the SA7025 airfoil. It is seen that for the SA7025 trips at all of the four locations reduce the C_d at $Re = 100{,}000$ over the range of C_l values where there is significant bubble drag. However, the magnitude of drag reduction at any particular C_l within this range depends on the location of the boundary-layertrip. At C_l values around 0.3, aft trip locations result in larger drag reduction owing to increased laminar flow. At C_l of around 0.8, the bubble has moved forward to around 0.4*c*. At this condition the aft trip locations become less effective in reducing the drag particularly when the laminar separation location is upstream of the trip. A more forward location of the trip is therefore more effective at C_l of 0.8. In contrast, for the $Re = 300{,}000$ case, where bubble drag is less dominant, the forward trip locations result in higher drag around C_l of 0.8 owing to greater loss in laminar flow. All of the trip locations show a reduction in C_d of approximately 0.001–0.002 over the clean airfoil case at $Re = 300{,}000$ and C_l in the range of 0 to 0.4. Examination of the results shows that the 0.4*c* trip location appears to be the most beneficial location for this airfoil. At this trip location there is a modest reduction in the bubble drag at $Re = 100{,}000$ along with a reduction in C_d at the low C_l values and the higher Reynolds number. In particular, at this trip location there is no degradation in performance when compared with that of the clean airfoil.

The effect of different trip locations on the SA7026 airfoil, shown in Figs. 15a–15d, is similar to that on the SA7025. At a C_l of around 0.4, the aft trip locations result in higher drag reductions at $Re = 100{,}000$ because of a greater loss in laminar flow when compared with the more forward trip locations. At C_l values in the vicinity of 0.8, the forward trip locations result in greater bubble drag reductions for $Re = 100{,}000$ because the trip is more upstream of the bubble. At the higher Reynolds number of 300,000, the forward trip locations result in an increase in the drag when compared with the clean airfoil because of increased skin friction resulting from loss in laminar flow. At the higher Reynolds numbers and lower C_l values of around 0.2, all of the trip locations result in a reduction in the drag over the clean airfoil. The optimum trip location for the SA7026 seems to be at 0.2*c*.

Comparison of the Tripped SA7026 with the Clean SA7024

In this subsection a comparison of lift and drag data is presented in order to assess whether or not it is possible to design a low Reynolds number airfoil with a trip to have overall better performance than an airfoil designed for good performance when clean. For this purpose, the SA7024 airfoil is taken as an example of an airfoil designed for good performance when clean. The performance of the clean SA7024 is compared with that of the tripped SA7026 in Fig. 16. Although the SA7026 has poor performance in the clean condition, the 0.2*c* trip location significantly improves the overall

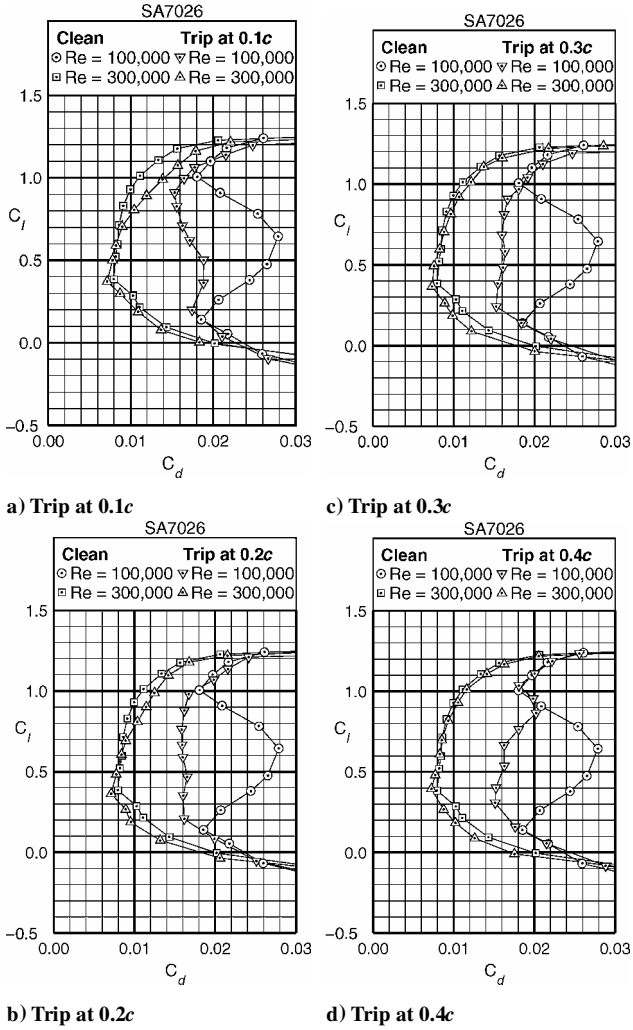

Fig. 15 Drag polars for the SA7026.

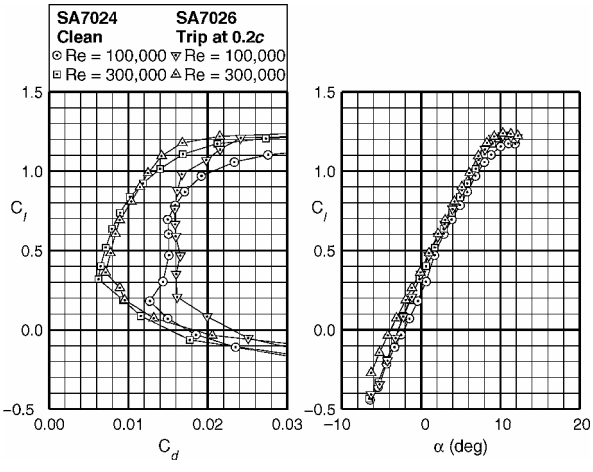

Fig. 16 Comparison of the 0.2*c*-tripped SA7026 with the clean SA7024.

performance of this airfoil. These results, therefore, serve as good examples of airfoils designed for good performance in the tripped condition using the design philosophy described in the preceding section.

In making the assessment, the differences in performance at the lower C_l are studied at the higher Reynolds number of 300,000, whereas the differences in the polars at the higher C_l are evaluated at the lower Reynolds number of 100,000. Such a comparison is necessary for a wing airfoil as it takes into account the change in Reynolds number as a result of changes in flight speed of an airplane in rectilinear flight.

Comparison of the polars in Fig. 16 shows that the tripped SA7026 airfoil has a noticeably better performance than the clean SA7024 at $Re = 100{,}000$ and C_l values of around 1.0. At the low C_l values of around 0.3, however, the tripped SA7026 has higher drag than the clean SA7024 at $Re = 300{,}000$. This shows that for the range of Reynolds numbers and airfoil shapes considered in this study, the design philosophy described in the preceding section has not resulted in a tripped airfoil with an uncompromised improvement over a clean airfoil at all flight conditions. The tripped airfoil does show an improvement at the high-C_l, lower Reynolds number condition, but this improvement is compromised by a small, but important loss in performance at the low-C_l, higher Reynolds number condition.

Conclusions

A study has been presented to assess whether it is possible to design low Reynolds number airfoils to make judicious use of both transition ramps and boundary-layer trips in order to achieve a better performance overall when compared to an airfoil designed for the clean condition. A design philosophy has been presented for designing low Reynolds number airfoils to have good performance in the tripped condition. For this study a series of three airfoils was designed with systematic changes to the shape of the transition ramp. The three airfoils were wind-tunnel tested at Reynolds numbers of 100,000 and 300,000 and at five conditions: clean, and with the trip located on the upper surface at 0.1*c*, 0.2*c*, 0.3*c*, and 0.4*c*.

An analysis of the results shows that for the Reynolds-number range and the airfoils considered in this study the airfoil optimized for the tripped condition has lower drag at the high-C_l, lower Reynolds number condition when compared with the airfoil optimized for clean performance. But this improvement is compromised by a small, but noticeable loss in performance at the low-C_l, higher Reynolds number condition. Thus, for the Reynolds numbers and airfoil shapes considered in the study, it was not possible to design an airfoil with trips to have a clear advantage over an airfoil designed for good performance in the clean condition. This study also confirms the perhaps well-known fact that for a given airfoil, a single trip location is not the optimum for different flight conditions. The wind-tunnel data gathered as a part of this systematic study, however, serves as a useful database for the development of empirical and computational methods for analysis of airfoils with trips.

It is also likely that a tripped airfoil can prove to be advantageous for design situations that need thicker airfoils than those considered in this study or where the operating Reynolds numbers are less than 100,000. At these conditions the dominant drag contribution is the pressure drag from the laminar separation bubble—the adverse effects of which are best mitigated by designing the airfoil to take advantage of boundary-layer trips. Owing to the lack of good airfoil analysis methods that can predict the effects of trips, airfoils designed to use trips currently need extensive and systematic wind-tunnel experimental investigation as a part of the design process. For this reason the study highlights the needs for the development of empirical and computational models that can account for the different effects of boundary-layer trips during the design stages of a low Reynolds number airfoil.

Acknowledgments

The authors wish to gratefully acknowledge Yvan Tinel, Tinel Technologies, for his efforts in the fabrication of the high-quality wind-tunnel models of the SA702x airfoils used in this work. Mark Drela is thanked for the XFOIL code used in this study.

References

[1] Wortmann, F. X., "Progress in the Design of Low Drag Airfoils," *Boundary Layer and Flow Control*, edited by G. V. Lachmann, London, 1961, pp. 748–770.

[2] Wortmann, F. X., "A Critical Review of the Physical Aspects of Airfoil Design at Low Mach Numbers," *Motorless Flight Research*, edited by J. L. Nash-Weber, NASA CR 2315, Nov. 1973, pp. 179–196.

[3]Drela, M., "Low Reynolds-Number Airfoil Design for the M.I.T. Daedalus Prototype: A Case Study," *Journal of Aircraft*, Vol. 25, No. 8, 1988, pp. 724–732.

[4]Maughmer, M. D., and Somers, D. M., "Design and Experimental Results for a High-Altitude, Long-Endurance Airfoil," *Journal of Aircraft*, Vol. 26, No. 2, 1989, pp. 148–153.

[5]Donovan, J. F., and Selig, M. S., "Low Reynolds Number Airfoil Design and Wind Tunnel Testing at Princeton University," *Low Reynolds Number Aerodynamics*, edited by T. J. Mueller, *Lecture Notes in Engineering*, Vol. 54, Springer-Verlag, New York, 1989, pp. 39–57.

[6]Eppler, R., *Airfoil Design and Data*, Springer-Verlag, New York, 1990.

[7]Selig, M. S., Gopalarathnam, A., Giguère, P., and Lyon, C. A., "Systematic Airfoil Design Studies at Low Reynolds Numbers," *Fixed and Flapping Wing Aerodynamics for Micro Air Vehicle Applications*, edited by T. J. Mueller, *Progress in Astronautics and Aeronautics*, Vol. 195, AIAA, Reston, VA, 2001, pp. 143–167.

[8]Carmichael, B., "Low Reynolds Number Airfoil Survey Volume 1," NASA CR 165803, Nov. 1981.

[9]Lissaman, P. B. S., "Low Reynolds Number Airfoils," *Annual Review of Fluid Mechanics*, Vol. 15, 1983, pp. 223–239.

[10]Selig, M. S., Donovan, J. F., and Fraser, D. B., *Airfoils at Low Speeds*, Soartech 8, SoarTech Publications, Virginia Beach, VA, 1989.

[11]Selig, M. S., Guglielmo, J. J., Broeren, A. P., and Giguère, P., *Summary of Low-Speed Airfoil Data, Vol. 1*, SoarTech Publications, Virginia Beach, VA, 1995.

[12]Selig, M. S., Lyon, C. A., Giguère, P., Ninham, C. N., and Guglielmo, J. J., *Summary of Low-Speed Airfoil Data, Vol. 2*, SoarTech Publications, Virginia Beach, VA, 1996.

[13]Lyon, C. A., Selig, M. S., and Broeren, A. P., "Boundary Layer Trips on Airfoils at Low Reynolds Numbers," AIAA Paper 97-0511, Jan. 1997.

[14]Lyon, C. A., Broeren, A. P., Giguère, P., Gopalarathnam, A., and Selig, M. S., *Summary of Low-Speed Airfoil Data*, Vol. 3, SoarTech Publications, Virginia Beach, VA, 1998.

[15]Althaus, D., *Profilpolaren für den Modellflug—Windkanalmessung an Profilen im Kritischen Reynoldszahlbereich*, Neckar-Verlag Villingen-Schwenningen, Germany, 1980.

[16]Mueller, T. J., and Batill, S. M., "Experimental Studies of the Laminar Separation Bubble on a Two-Dimensional Airfoil at Low Reynolds Numbers," *AIAA Journal*, Vol. 20, No. 4, 1982, pp. 457–463.

[17]Bloch, D. R., and Mueller, T. J., "Effects of Distributed Grit Roughness on Separation and Transition on an Airfoil at Low Reynolds Numbers," AIAA Paper 86-1788, 1986.

[18]Huber, A. F., and Mueller, T. J., "The Effect of Grit Roughness on the Performance of the Wortmann FX 63-137 Airfoil at a Chord Reynolds Number of 100,000," *Proceedings of the Aerodynamics at Low Reynolds Numbers* $10^4 < Re < 10^6$ *International Conference*, The Royal Aeronautical Society, London, Vol. 3, Paper 28, 1986, pp. 28.1–28.16.

[19]Boermans, L. M. M., Duyvis, F. J. D., van Ingen, J. L., and Timmer, W. A., "Experimental Aerodynamic Characteristics of the Airfoils LA 5055 and DU 86-084/18 at Low Reynolds Numbers," *Low Reynolds Number Aerodynamics*, edited by T. J. Mueller, *Lecture Notes in Engineering*, Vol. 54, Springer-Verlag, New York, 1989, pp. 115–130.

[20]Johnson, R. H., "Are Your Turbulators Too Large?" *Soaring*, Jan. 1995, pp. 29–31.

[21]Nayfeh, A. H., and Ragab, S. A., "Effect of Roughness on the Stability of Boundary Layers," AIAA Paper 86-1044, May 1986.

[22]Danabasoglu, G., Biringen, S., and Streett, C. L., "Spatial Simulation of Boundary Layer Instability: Effects of Surface Roughness," AIAA Paper 93-0075, Jan. 1993.

[23]Selig, M. S., and Maughmer, M. D., "A Multi-Point Inverse Airfoil Design Method Based on Conformal Mapping," *AIAA Journal*, Vol. 30, No. 5, 1992, pp. 1162–1170.

[24]Selig, M. S., and Maughmer, M. D., "Generalized Multipoint Inverse Airfoil Design," *AIAA Journal*, Vol. 30, No. 11, 1992, pp. 2618–2625.

[25]Drela, M., "XFOIL: An Analysis and Design System for Low Reynolds Number Airfoils," *Low Reynolds Number Aerodynamics*, edited by T. J. Mueller, *Lecture Notes in Engineering*, Vol. 54, Springer-Verlag, New York, 1989, pp. 1–12.

[26]Guglielmo, J. J., and Selig, M. S., "Spanwise Variations in Profile Drag for Airfoils at Low Reynolds Numbers," *Journal of Aircraft*, Vol. 33, No. 4, 1996, pp. 699–707.

[27]Guglielmo, J. J., "Spanwise Variations in Profile Drag for Airfoils at Low Reynolds Numbers," Master's Thesis, Univ. of Illinois at Urbana–Champaign, Dept. of Aeronautical and Astronautical Engineering, Urbana, IL, May 1995.

[28]Rae, W. H., Jr., and Pope, A., *Low-Speed Wind Tunnel Testing*, Wiley, New York, 1984, pp. 93–95, 344–362.

[29]Giguère, P., and Selig, M. S., "Freestream Velocity Measurements for Two-Dimensional Testing with Splitter Plates," *AIAA Journal*, Vol. 35, No. 7, 1997, pp. 1195–1200.

[30]McGhee, R. J., Walker, B. S., and Millard, B. F., "Experimental Results for the Eppler 387 Airfoil at Low Reynolds Numbers in the Langley Low-Turbulence Pressure Tunnel," NASA TM 4062, Oct. 1988.

[31]Coleman, H. W., and Steele, W. G., Jr., *Experimentation and Uncertainty Analysis for Engineers*, Wiley, New York, 1989.